

# A novel nitidine chloride nanoparticle overcomes the stemness of CD133 + EPCAM + Huh7 Hepatocellular Carcinoma Cells for liver cancer therapy

Danni Li (✉ [2742657328@qq.com](mailto:2742657328@qq.com))

Guangxi University for nationalities

Qiyang Zhang

Guangxi University for nationalities

Yuzhu Zhou

Guangxi University for nationalities

Hua Zhu

Guangxi University for Chinese medicine

Tong Li

Guangxi University for Chinese medicine

Fangkai Du

Guangxi University for nationalities

---

## Research Article

**Keywords:** Nitidine chloride nanoparticles, EpCAM+ /CD133+ Huh7 cells, AQP3/STAT3/CD133 pathway, Huh7 cells xenograft nude mice

**Posted Date:** April 8th, 2022

**DOI:** <https://doi.org/10.21203/rs.3.rs-1481834/v1>

**License:**   This work is licensed under a Creative Commons Attribution 4.0 International License.

[Read Full License](#)

---

# Abstract

**Background:** Stemness of CD133<sup>+</sup>EPCAM<sup>+</sup> hepatocellular carcinoma cells ensures cancer resistance to apoptosis, which is a challenge to current liver cancer treatments. Here we discovered that a novel nitidine chloride nanoparticle (TPGS-FA/NC, TPGS-FA: folic acid modified D- $\alpha$ -tocopheryl polyethylene glycol 1000 succinate, NC: nitidine chloride) targeted Huh7 human hepatocellular carcinoma and promoted its apoptosis in mice and cells. CD133 expression regulates AQP3 expression, promoting to increase the stemness properties of hepatoma cells. Importantly, AQP3 is associated with stimulation and nuclear translocation of STAT3 with an increasing expression level of CD133.

**Methods:** Cell viability was assessed by MTT and colony assays. TPGS-FA/NC nanoparticles were assayed by using confocal microscopy targeting Huh7 Hepatocellular Carcinoma Cells. A sphere culture technique was used to enrich cancer stem cells (CSC) and sort the CD133<sup>+</sup>EPCAM<sup>+</sup> Huh 7 cells by magnetic-activated cell sorting assay. The proteins were examined by immunohistochemistry and western blotting assay.

**Result:** TPGS-FA/NC nanoparticles reduced the CD133<sup>+</sup>EPCAM<sup>+</sup> Huh7 cells numbers in vitro. Furthermore, its time-dependently suppressed the AQP3/CD133/STAT3/JAK signaling pathways. Nitidine chloride nanoparticles therapy prevented and treated hepatocellular carcinoma in mice without adverse effects.

**Conclusions:** TPGS-FA/NC is shown to be a promising and safe drug against liver cancer therapy via AQP3/STAT3/CD133 axis.

## Background

Multiple drugs have been used broadly in liver cancer therapy, but their water-insolubility and toxicity have raised serious concerns [1,2]. Nitidine chloride has been developed in the past two decades due to its promising pharmacological action. Nitidine chloride promises therapeutic efficiency but often faces challenges due to potential organ damage, hypersensitivity, and neurotoxicity [3,4].

The cancer stem cells (CSC) are identified as stem cell properties, which revealed the existence of CSC in HCC [5,6]. CD133<sup>+</sup>EPCAM<sup>+</sup> phenotype precisely represented the characteristics of CSC in Huh7 cells [7–11]. Currently, some chemotherapeutic drugs primarily inhibit the growth of differentiated tumor cells with no impact on CSC [12–13]. Cancer stem cells (CSCs) maintain the stemness to ensure their survival and growth, and become resistant to current treatments [14–16]. The intrinsic pathway of CD133<sup>+</sup>Huh7 cells is regulated by the AQP3 protein in the progression and metastasis of several malignant tumors [17–20]. Furthermore, Nek2 is the critical regulator of the centrosome, making hepatocellular carcinoma more resistant to current treatments [21].

Based on the understanding that hepatocellular carcinoma contains functional AQP3 and Nek2 is mutated or highly expressed, these survival mechanisms can be overcome by the pharmacological action

of AQP3/STAT3/CD133 pathway degradation and Nek2 inhibition. Furthermore, Our findings investigate the combination of direct AQP3/STAT3/CD133 pathway and Nek2 protein inhibition as a novel nitidine chloride nanoparticle therapeutic strategy that can promote cancer stem cells apoptosis in hepatocellular carcinoma. we addressed the nitidine chloride nanoparticle therapeutic potential in vitro and in vivo

## Methods

### Materials

TPGS-FA/NC was synthesized in our laboratory and dissolved in DMSO. DMEM was purchased from Life Technologies (AB & Invitrogen)(Gibco, Suzhou, China). Fetal bovine serum (FBS) was purchased from Gemini (Gemini Calabasas, CA, USA). Huh7 was purchased from Procell Life Science & Technology Co. Ltd. on July 11, 2019 (identification number: CL-0120, Wuhan, China). Recombinant human bFGF (bFGF) and MTT were purchased from Beijing Solarbio Science & Technology Co., Ltd.(Solarbio, Beijing, China) and recombinant human 1 epidermal growth factor (EGF) were acquired from Shanghai Yuanye Biotechnology Corporation (Yuanye, Shanghai, China). were purchased from Procell Science&Technology Co.,Ltd.(Procell,Wuhan, China) .B27 (×50) were purchased from ThermoFisher Scientific( ThermoFisher, Waltham, USA). DMEM/F-12, insulin-Transferrin-Selenium (ITS×100), L-glutamine (×100) were purchased from Procell Science&Technology Co.,Ltd.(Procell,Wuhan, China). Anti-CD133 (AC133)-phycoerythrin (PE) and anti-CD326 (EpCAM)-allophycocyanin (APC) antibodies and isotype-matched mouse anti-IgG1-PE and anti-IgG1-APC were purchased from MiltenyiBiotec (North Rhine-Westphalia, Germany). Anti-phosphoSTAT3 (Tyr705), STAT3, JAK1, JAK2, AQP3, EpCAM, NEK2 were purchased from the Beijing Solarbio Science & Technology Co., Ltd. (Solarbio, Beijing, China). Anti-CD133 and anti-GAPDH were purchased from the Procell Science&Technology Co.,Ltd.(Procell,Wuhan, China). Anti-rabbit secondary antibodies were purchased from Thermo Fisher Scientific Science&Technology Co.,Ltd.(Thermo Fisher Scientific, Shanghai, China). DAPI was obtained from Shanghai Beyotime Biotechnology Co. Ltd. (Beyotime, Shanghai, China). TheiFluor™ 647 phalloidin iFluor™ were purchased from Yeasen Biotechnology Co., Ltd.(Yeasten, Shanghai, China). 5-fluorouracil (5-Fu) was purchased from MedChemExpress (MCE, Monmouth Junction, NJ, USA).

### Cell culture

Huh7 cells were cultured in DMEM 10% FBS containing 10% FBS, 100 U/mL penicillin, and 50 mg/mL streptomycin at 37 °C in a humidified 5% CO<sub>2</sub> incubator.

### Tumor sphere formation assay and flow cytometric analysis

Primary sphere cells were obtained by culturing Huh7 cells in sphere-forming conditioned DMEM/F12, supplemented with FGF (20 ng/mL), EGF (20 ng/mL), B27 (1×), and L-glutamine (1×) in 6-well ultra-low attachment plates. The primary sphere cells (1×10<sup>3</sup> cells/well) were incubated with or without TPGS-FA/NC for 7d. The second and third passages of the cells were grown for 7 d in the absence of TPGS-FA/NC. To examine TPGS-FA/NC effects on the subpopulation of cells that expressed

EpCAM and CD133, cells were incubated with anti-AC133-PE and anti-EpCAM-APC antibodies and analyzed by flow cytometry. Isotype-matched mouse anti-IgG1-PE and anti-IgG1-APC were used as controls.

### **Confocal microscopy imaging**

Huh7 cells were seeded on glass cover-slips and cultured at 37 °C overnight. Rhodamine B isothiocyanate 540-labeled TPGS-FA/NC were incubated with cells at a final concentration of 100 nM for 4h at 37 °C. After washing twice with PBS buffer, cells were fixed with 4% formaldehyde and washed again, followed by treatment with 0.1% Triton X-100 in PBS buffer for 5min and subsequent cytoskeleton staining with iFluor™ 647 phalloidin iFluor™ for 30 min at room temperature, containing DAPI for cell nucleus staining and assayed on Leica SP8 confocal microscope (Leica Corp.).

### **Western blotting**

Cells were lysed in RIPA lysis buffer with PMSF and protease inhibitors. Total protein lysates were boiled with loading sample buffer containing 8% SDS-PAGE. Separated proteins were transferred onto PVDF membranes. PVDF membrane blots were blocked in 10% skimmed milk for 0.5-1h at room temperature, washed in Tris-buffered saline with Tween 20 (TBS-T) and incubated overnight at 4°C with rabbit anti-phosphoSTAT3 (Tyr705), anti-STAT3, anti-JAK1, anti-JAK2, anti-AQP3 CD33, anti-GAPDH. Anti-rabbit IgG was used as the second antibody.

### **Immunohistochemistry (IHC)**

AQP3/CD133/EPCAM/NEK2 expression was analyzed in paraffin-embedded specimens obtained from nude mice tumor tissue. Tissue sections were incubated with anti-AQP3 (1:100, Solarbio), anti-CD133 (1:100, Solarbio), anti-EPCAM (1:100, Solarbio), and anti-NEK2 (1:100, Solarbio) overnight at 4°C. Then, the sections were incubated with biotinylated goat anti-rabbit IgG as a secondary antibody (Zhongshan Kit, China) for 30 min at 37°C. The specimens were assessed three times.

### **In vivo biodistribution assay.**

Rhodamine B isothiocyanate-labeled TPGS-FA/NC (2mg.kg<sup>-1</sup>, NC per body weight) were systemically administered via the tail vein into Huh7 tumor-bearing mice. PBS-injected mice were used as fluorescence negative controls. The whole-body imaging of mice was conducted at 8h using an IVIS system (XMRS) with excitation at 535 nm and emission at 694 nm. The mice were sacrificed at 8h post-injection by the inhalation of CO<sub>2</sub> followed by cervical dislocation, and major organs were collected and subjected to fluorescence imaging for the assessment of biodistribution profiles. The fluorescence imaging data of average radiant efficiency ( [ps<sup>-1</sup>cm<sup>-2</sup>sr<sup>-1</sup>] [μWcm<sup>-2</sup>]<sup>-1</sup> ) were quantitative by IVIS system (XMRS) program.

### **Magnetic-activated cell sorting assay.**

Determine cell number, Centrifuge cell suspension at 300×g for 10 minutes, Aspirate supernatant completely. Resuspend cell pellet in 300µL of buffer per 5×10<sup>7</sup> total cells. Add 100µL of FcR Blocking Reagent per 5×10<sup>7</sup> total cells and mix well. Add 100µL of EpCAM microbeads per 5×10<sup>7</sup> total cells. Mix well and incubate for 30 minutes in the refrigerator (2–8°C). Wash cells by adding 5–10 mL of buffer per 5×10<sup>7</sup> cells and centrifuge at 300×g for 10 minutes. Aspirate supernatant completely and suspend up to 10<sup>6</sup> cells in 500µL buffer, proceed to magnetic separation, EpCAM Huh7 cells were collected. Followed above methods, EpCAM Huh7 cells were sorted after CD133 microbeads incubation. EpCAM<sup>+</sup> and CD133<sup>+</sup> Huh7 cells were collected by magnetic separation.

### **In vivo tumor inhibition by TPGS-FA/NC nanoparticles.**

Freshly sorted CD133<sup>+</sup>EpCAM<sup>+</sup> cells were collected in sterile DMEM without FBS. 200µL cell suspension, mixed with matrigel (BD Biosciences, CA) (1:1), was subcutaneously injected into each BALB/c nude mice, which were randomly divided into four groups (n=5 biologically independent animals). Samples were administered by i.v. injection in a total of 5 doses (4mg kg<sup>-1</sup>, NC per body weight) every other day. Tumor volume, calculated as (length×width<sup>2</sup>)/2, and mouse weight were monitored every other day. Data were statistically analyzed by two-tailed unpaired t-test and presented as mean ± SD; \*p < 0.05; \*\*p < 0.01; \*\*\*p < 0.001.

**Statistics.** Statistical differences were evaluated using two-tailed unpaired t-test with GraphPad software, and statistically significant differences are denoted as \*p < 0.05, \*\*p < 0.01, and \*\*\*p < 0.001. No adjustments were made for multiple comparisons.

## **Results**

### **TPGS-FA/NC inhibited cell proliferation and targeted the Huh7 cells**

Huh7 cells (2×10<sup>3</sup> cells/well) were seeded into 96-well plates and treated with TPGS-FA/NC (0–120 µg/mL) for 24, 48, and 72h (Fig. 1). Cell proliferation was assessed using MTT in a concentration- and time-dependent manner. To evaluate nanoparticles targeting tumor capability, the Rhodamine B isothiocyanate 540 fluorophore was attached to TPGS-FA. Confocal microscope imaging showed that TPGS-FA/NC nanoparticles entered the Huh7 cells in vitro, compared with the control groups (Fig. 2).

### **TPGS-FA/NC reduced hepatic cancer stem-like cells**

To investigate whether TPGS-FA/NC suppressed hepatic CSCs, we enriched the hepatic CSC populations in the Huh7 cell lines using the sphere culture technique. The flow cytometric analysis demonstrated that the EpCAM<sup>+</sup>/CD133<sup>+</sup> cells accounted for 82.0% of the Huh7 sphere cells, respectively. TPGS-FA/NC (10, 20 and 40µg/mL) potentially reduced the fraction of EpCAM<sup>+</sup>/CD133<sup>+</sup> cells (Fig. 3a).

### **TPGS-FA/NC inhibited hepatoma cell proliferation and colony formation**

HCC cells ( $1 \times 10^3$  cells/well) were treated with or without TPGS-FA/NC in 6-well ultra-low attachment microplates and allowed to grow for 17 to 21 days. The TPGS-FA/NC treatment inhibited Huh7 cell proliferation and also markedly reduced the number of colonies in the clonogenic assays (Fig. 3b).

### **TPGS-FA/NC suppressed the AQP3 /CD133/STAT pathways**

TPGS-FA/NC reduced the protein expression levels of JAK1, JAK2, pY705-STAT3, STAT3 (Fig. 4). Furthermore, TPGS-FA/NC reduced the AQP3 protein expression, which suppressed the expression of activated STAT3 (pY705-STAT3) (Fig. 4). Then, in vivo experiment, we tested the CD133 and AQP3 expression levels in sections of nude mice subcutaneous tumors by IHC, results showed TPGS-FA/NC downregulated AQP3 and CD133 protein levels (Fig. 5).

### **TPGS-FA/NC impaired NEK2/CD133/EpCAM signaling of HCC**

The protein levels of NEK2, CD133 and EpCAM were determined in cells and nude mice treated with and without TPGS-FA/NC. TPGS-FA/NC successfully reduced protein expression levels of NEK2, CD133 and EpCAM in HCC. In vivo experiment, we tested the CD133 and AQP3 expression levels in sections of nude mice subcutaneous tumors by IHC, results showed TPGS-FA/NC downregulated NEK2, CD133 and EpCAM protein levels (Fig. 5).

### **In vivo significant inhibition of tumor by TPGS-FA/NC nanoparticles**

Tumor quantitative biodistribution and targeting of the TPGS-FA/NC were assessed, which were injected through the tail vein in vivo. Those images of mice 8h post-injection showed that the TPGS-FA/NC nanoparticles markedly accumulated in tumor, with low or no accumulation in brain, heart, spleen. (Fig. 6a). Quantitative analysis of the organ images showed strongly tumor accumulation. (Fig. 6b). After injecting with TPGS-FA/NC at a dose of  $4 \text{ mg kg}^{-1}$  (NC per mouse weight) every 2 days for a total of five dosages, the results revealed an inhibitory capability in vivo as administration by tumor volumes, whereas control group (Fig. 6c). The specific tumor inhibition was further confirmed from the tumors harvested after 2-week post injections (Fig. 6d). Those nanoparticles were biocompatible, which showed no obvious organ toxicity over two-week post injections (Fig. 7).

## **Discussion**

In this study, TPGS-D- $\alpha$ -tocopheryl polyethylene glycol 1000 succinate is a very safe biocompatible and safe agent that can efficiently be used as a drug solubilizer [23,24]. Previously, we reported the folic acid modified D- $\alpha$ -tocopheryl polyethylene glycol 1000 succinate (TPGS-FA) as a potential carrier for controlled delivery [25].

Our studies suggest that populations of hepatic cancer stem cells self-renewal capacities with expressed biomarkers (EpCAM and CD133). TPGS-FA/NC demonstrated markedly decreased the positive EpCAM/CD133 cell spheres population, and numbers and sizes. The fact that our studies in vivo reveal

atherapeutic efficacy with adose of 4 mgkg<sup>-1</sup> treatment for 14d significantly inhibited Huh7 xenograft tumor growth and overall a safe profile in organ , is noteworthy. CD133 represents Liver cancer stem cells (LCSCs) marker with promoting HCC proliferation and invasion[26-28].Previous evidence has shown that high expression levels of AOP3 exerted carcinogenic and therapy resistance with promoting hepatocellular carcinoma formation[29].Importantly, our work addresses a promising chemotherapeutic drug delivery by using theTPGS-FA with thecapabilities of nitidinechloride, tumor targeting for liver cancer therapy.

## **Conclusion**

TPGS-FA/NC significantly inhibit Huh7 cellular proliferation and colony formation. TPGS-FA/NC suppressed the AQP3/CD133/STAT3 pathway with reducing expression of phosphorylation STAT3, its upstream factor (AQP3) and two downstream signaling molecules (JAK1 and JAK2) . In this study, Our findings demonstrate TPGS-FA/NC therapeutic effects in vitro and in vivo. The work offer preclinical proof-of-concept for the treatment of a new intravenously bioavailable AOP3 inhibitor, nitidine chloridenanoparticles, which may provide a broad therapeutic effect in liver cancer.

## **Declarations**

### **Ethics Approval and Consent to Participate**

This study was approved by Ethics Committee of Guangxi University for Chinese medicine, all procedures reporting in this study on the animals were carried in accordance with the ARRIVE guidelines, and the study was carried out in accordance with the relevant guidelines and regulations. Huh 7 human hepatocellular carcinoma line did not require ethics approval for their use. Informed consent was therefore not applicable.

### **Consent for publication**

Not applicable.

### **Availability of data and materials**

All data generated or analyzed during the present study are included in this article. supplementary data are present in the supplemental materials. Additional data related to this paper can be requested from the author (2742657328@qq. com).

### **Competing interests**

The authors declare that they have no competing interests.

### **Funding**

This work was supported by the Guangxi Natural Science Foundation (2017GXNSFBA198021), Guangxi Key Laboratory of Zhuang and Yao Ethnic Medicine ((2014) No.32), Collaborative Innovation Center of Zhuang and Yao Ethnic Medicine ((2013) No.20), and the Guangxi University for Nationalities Key Laboratory of National Medicine ,Natural Science Foundation of China(No.11904059).

## Acknowledgments

We are grateful to professor Bernard at Guangxi University for revising the manuscript.

## Authors' contribution

D. L. and H.Z. and T.L. and F.D. designed the main manuscript and D.L. and Q.Z. and Y.Z. prepared the experiments and prepared figures 1-7. All authors reviewed the manuscript.

## Author's information

<sup>1</sup>School of Chemistry and chemical engineering, Guangxi Key Laboratory for Polysaccharide Materials and Modifications, Guangxi University for nationalities, No.158, Da Xue Xi street, Xixiangtang District, Nanning 530006, Guangxi Province, China. <sup>2</sup>College of Pharmacy, Guangxi University for Chinese medicine, No.13, Wu He street, Qingxiu District, Nanning, 530200, Guangxi Province, China.

## References

1. Spencer, C. M. & Faulds, D. Paclitaxel. A review of its pharmacodynamic and pharmacokinetic properties and therapeutic potential in the treatment of cancer. *Drugs* 48, 794–847 (1994).
2. Rowinsky, E. K. & Donehower, R. C. Paclitaxel (taxol). *N. Engl. J. Med.* 332, 1004–1014 (1995).
3. Li L, Tu M, Yang X, Sun S, Wu X, Zhou H, et al. The contribution of human OCT1, OCT3, and CYP3A4 to nitidine chltoxicity. *Drug Metab Dispos.* 2014;42:1227–34.
4. Li LP, Song FF, Weng YY, Yang X, Wang K, Lei HM, Ma J, Zhou H, Jiang HD. Role of OCT2 and MATE1 in renal disposition and toxicity of nitidine chloride. *Br J Pharmacol.* 2016;173:2543–54.
5. Jemal A, Bray F, Center MM, et al. Global cancer statistics. *CA Cancer J Clin.* 2011; 61: 69-90.
6. Zhou BB, Zhang H, Damelin M, et al. Tumour-initiating cells: challenges and opportunities for anticancer drug discovery. *Nat Rev Drug Discov.* 2009; 8: 806-823.
7. Reya T, Morrison SJ, Clarke MF, Weissman IL. Stem cells, cancer, and cancer stem cells. *Nature* 2001; 414: 105–11.
8. Ma S, Chan KW, Hu L, Lee TK, Wo JY, Ng IO, et al. Identification and characterization of tumorigenic liver cancerstem/progenitor cells. *Gastroenterology* 2007; 132: 2542–56.
9. Yamashita T, Honda M, Nakamoto Y, Baba M, Nio K, Hara Y, et al. Discrete nature of EpCAM+ and CD90+ cancer stem cells in human hepatocellular carcinoma. *Hepatology* 2013; 57: 1484–97.



10. Yamashita T, Ji J, Budhu A, Forgues M, Yang W, Wang HY, et al. EpCAM-positive hepatocellular carcinoma cells are tumor-initiating cells with stem/progenitor cell features. *Gastroenterology* 2009; 136: 1012–24.
11. Xu X, Liu RF, Zhang X, Huang LY, Chen F, Fei QL, et al. DLK1 as a potential target against cancer stem/progenitor cells of hepatocellular carcinoma. *Mol Cancer Ther* 2012; 11: 629–38.
12. Yi Chen, Dongke Yu, Hao Zhang , et al. CD133+EpCAM+ Phenotype Possesses More Characteristics of Tumor Initiating Cells in Hepatocellular Carcinoma Huh7 Cells .*International Journal of Biological Sciences* 2012; 8(7):992-1004.
13. Ying LIU, Yang QI2 , Zhi-hui BAI, Chen-xu , et al. A novel matrine derivate inhibits differentiated human hepatoma cells and hepatic cancer stem-like cells by suppressing PI3K/AKT signaling pathways. *Acta Pharmacologica Sinica* (2017) 38: 120–132
14. Zhou,Y.etal.Aquaporin3 promotes the stem-like properties of gastric cancer cells via Wnt/GSK-3 $\beta$ / $\beta$ -catenin pathway.*Oncotarget*.7,16529–16541(2016).
15. Juuti Uusitalo, K. et al. Aquapor in expression and function in human pluri potent stem cell-derived retinal pigment edepithelial cells . *Invest.Ophthalmol.Vis.Sci*.54,3510–3519(2013).
16. Ya wei Wang ,Gang Wu,Xue yan Fu et al. Aquaporin3 maintains the stemness of CD133<sup>+</sup>hepatocellular carcinoma cells by activating STAT3.
17. Wang , X.et al. AQP3 small interfering RNA and PLD2 small interfering RNA inhibit the proliferation and promote the apoptosisof squamous cell carcinoma. *Mol.Med.Rep*.16,1964–1972(2017).
18. Huang , X., Huang, L.&Shao,M. Aquaporin 3 facilitates tumor growth in pancreatic cancer by modulating mTOR signaling .*Biochem. Biophys. Res.Commun*.486 ,1097–1102(2017).
19. Xiong,G.etal.RNA interference influenced the proliferation and invasion of XWLC-05 lung cancer cells through inhibiting aquaporin3. *Biochem.Biophys.Res.Commun*.485,627–634(2017).
20. Graziano,A.C.E.,Avola,R.,Pannuzzo,G.&Cardile,V.Aquaporin1and3 modification as a result of chondrogenicdifferentiationofhumanmesenchymalstemcell.*J.CellPhysiol*.233,2279–2291(2018).
21. Wu W, Baxter JE, Wattam SL, Hayward DG, Fardilha M, KnebelA, Ford EM, da Cruz e Silva EF and Fry AM: Alternative splicing controls nuclear translocation of the cell cycle-regulated Nek2 kinase. *J Biol Chem* 282: 26431-26440, 2007.
22. LiuX, GaoY, LuY,ZhangJ,LiL,YinF. Up regulation of NEK2 is associated with drug resistance in ovarian cancer.*Oncol.Rep*.2014;3 1:745–54.
23. Varma MVS, Panchagnula R. Enhanced oral paclitaxel absorption with vitamin E TPGS: effect on solubility and permeability in vitro, in situ and in vivo. *Eur J Pharm Sci*. 2005;25:445–53.
24. Collnot EM, Baldes C, Schaefer UF, Edgar KJ, Wempe MF, Lehr CM. Vitamin E TPGS p-glycoprotein inhibition mechanism: influence on conformational flexibility, intracellular ATP levels, and role of time and site of access. *Mol Pharm*. 2010;7:642–51.
25. Danni Li,Shaogang Liu, JiahaoZhu . Folic acid modified TPGS as a novel nanomicelle for delivery of nitidine chloride to improve apoptosis induction in Huh7 human hepatocellular carcinoma. *BMC*

26. Tang, K. H. et al. CD133(+) liver tumor-initiating cells promote tumorangiogenesis, growth, and self-renewal through neurotensin/interleukin-8/CXCL1 signaling. *Hepatology* 55, 807–820 (2012).
27. Kohga, K. et al. Expression of CD133 confers malignant potential by regulating metalloproteinases in human hepatocellular carcinoma. *J Hepatol.* 52, 872–879 (2010).
28. Wang, X. et al. Insufficient radiofrequency ablation promotes hepatocellular carcinoma cell progression via autophagy and the CD133 feedback loop. *Oncol. Rep.* 40, 241–251 (2018).
29. Yawei ,W. et al. Aquaporin 3 maintains the stemness of CD133+ hepatocellular carcinoma cells by activating STAT3. *Cell Death and Disease* (2019) 10:465-480.

## Figures

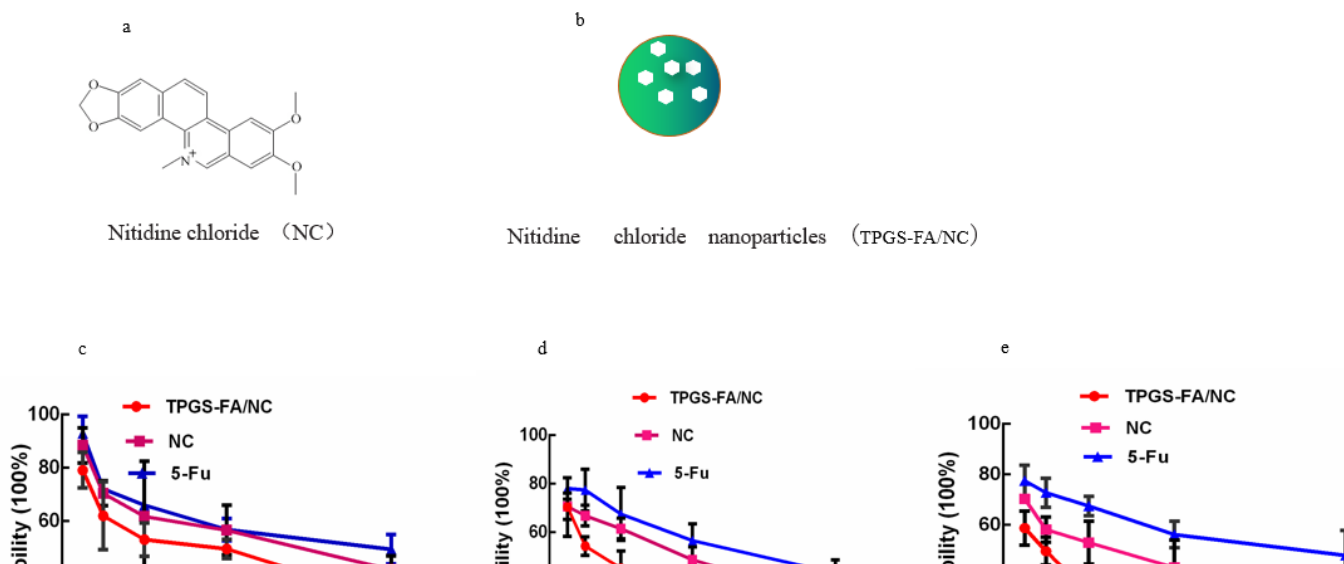


Figure 1

The effect of TPGS-FA/NC on Huh7 cell proliferation and colony formation. (a) Chemical structure of NC (b) TPGS-FA/NC nanoparticles. (c-e) TPGS-FA/NC inhibited Huh7 cell proliferation as determined by the MTT assay in 24, 48 and 72h.  $n=3$ .  $*P<0.05$  vs control.

Figure 2

In vitro Huh7 cells binding of TPGS-FA/NC nanoparticles, shown by confocal microscopy (blue: nucleus; green: cytoskeleton; red: TPGS-FA/NC nanoparticles. Scale bar: 50  $\mu\text{m}$  for original images, and 10  $\mu\text{m}$  for magnified image).

Figure 3

The effect of TPGS-FA/NC on hepatic cancer stem-like cells. a. TPGS-FA/NC reduced the population of EpCAM<sup>+</sup>/CD133<sup>+</sup> cells in the spheres treated with TPGS-FA/NC for 48h. b. TPGS-FA/NC reduced the sizes Huh7 primary spheres (magnification,  $\times 400$ ).

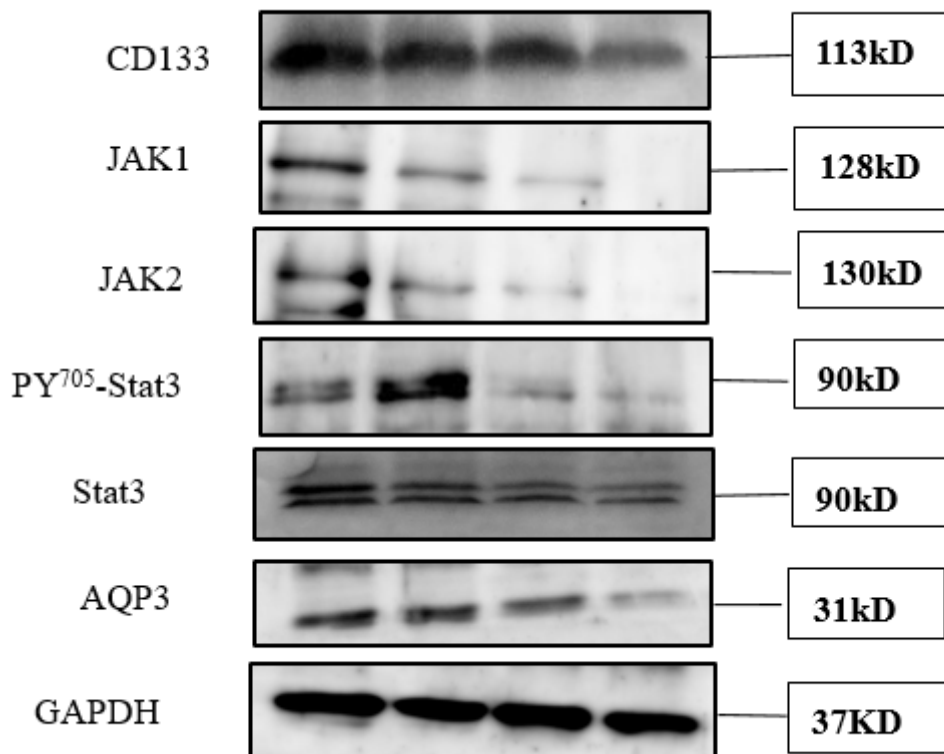


Figure 4

TPGS-FA/NC nanoparticles regulates CD133 and PY705-STAT3 protein by AQP3 proteins Expression of (DMSO  $\square$  TPGS-FA/NC: 10  $\mu\text{g/mL}$   $\square$  20  $\mu\text{g/mL}$   $\square$  40  $\mu\text{g/mL}$ )

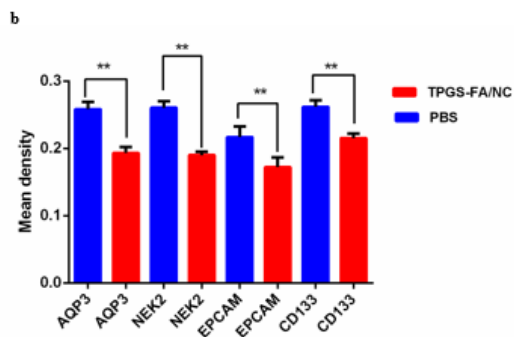
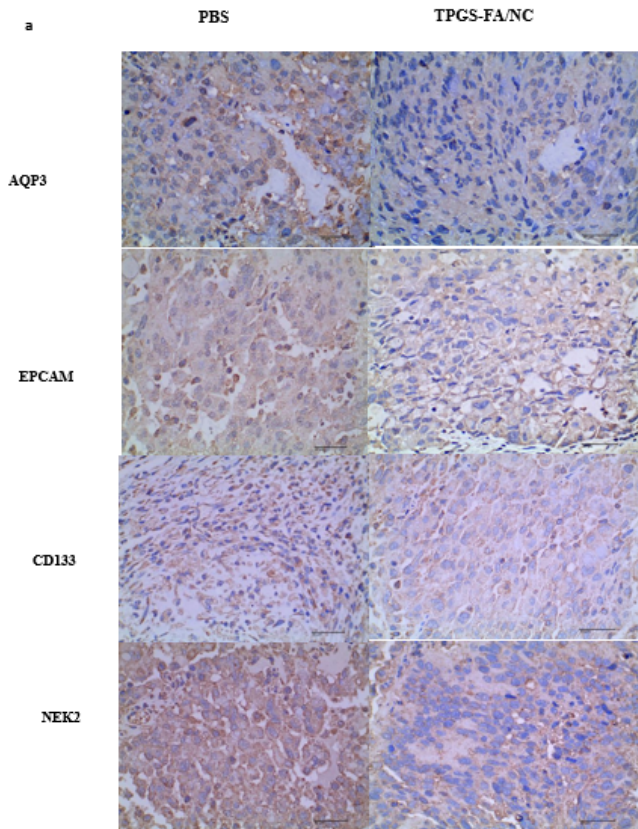


Figure 5

a. The protein of AQP3 , NEK2,EPCAM, and CD133 ( $\times 400$ ,  $40\mu\text{m}$ ) were mainly located in cytomembrane according to IHC in Huh7 cells. b.The protein expression of AQP3 , NEK2,EPCAM, and CD133 ( $\times 200$ ) were mainly located in cytomembrane according to IHC in 25 HCC mice bearing Huh7 xenograft specimens  $***p < 0.01$

## Figure 6

a. Representative organ images showing specific tumor targeting of rhodamine B isothiocyanate labeled TPGS-FA/NC nanoparticles 8 h post-injection into mice bearing Huh7 xenograft (T: tumor, Li: liver, H: heart, L: lung, K: kidney, S: spleen, and B: brain; Color scale: radiant efficiency, [ $\mu\text{Wcm}^{-2}$ ] $^{-1}$ ). V b. Quantitative analysis of biodistribution in tumors and normal organs, quantified from the organ images. Intravenous treatment of nude mice bearing orthotopic Huh7 xenografts with TPGS-FA/NC nanoparticles (red) and control groups (turquoise: NC, fuchsia: 5-Fu, blue: PBS) every other day for a total of five injections (4 mg kg<sup>-1</sup>, NC per body weight, indicated by arrows). c. Mice body weight was monitored during the time course of treatments (n = 5 biologically independent animals, statistics was calculated by two-tailed unpaired t-test presented as mean  $\pm$ SD, \*p < 0.05, \*\*p < 0.01, \*\*\*p < 0.001; p =  $4.3 \times 10^{-3}$ ,  $3.4 \times 10^{-3}$  and  $5.0 \times 10^{-4}$  comparing TPGS-FA/NC to NC, 5-Fu and PBS, respectively). d. Representative images of liver cancer tumors harvested from mice after treatments \*p < 0.05, \*\*p < 0.01, \*\*\*p < 0.001; p = 0.01,  $8 \times 10^{-4}$ , and  $2 \times 10^{-4}$  comparing TPGS-FA/NC to NC, 5-Fu, and PBS, respectively. Source data are provided as a Source Data file.

## Figure 7

HE stained in 20 HCC mice bearing Huh7 xenograft specimens

## Supplementary Files

This is a list of supplementary files associated with this preprint. Click to download.

- [SupplementaryInfoFile.pdf](#)
- [Supplementarymaterial.pdf](#)